Studies on effects of feedback delay on the convergence performance of adaptive time-domain equalizers for fiber dispersive channels

Qun Guo
Bo Xu
Kun Qiu

Studies on effects of feedback delay on the convergence performance of adaptive time-domain equalizers for fiber dispersive channels

Qun Guo, Bo Xu,* **and Kun Qiu**
University of Electronic Science and Technology of China, School of Communication and Information Engineering, Key Laboratory of Optical Fiber Sensing and Communications (Education Ministry of China), Chengdu 611731, China

Abstract. Adaptive time-domain equalizer (TDE) is an important module for digital optical coherent receivers. From an implementation perspective, we analyze and compare in detail the effects of error signal feedback delay on the convergence performance of TDE using either least-mean square (LMS) or constant modulus algorithm (CMA). For this purpose, a simplified theoretical model is proposed based on which iterative equations on the mean value and the variance of the tap coefficient are derived with or without error signal feedback delay for both LMS- and CMA-based methods for the first time. The analytical results show that decreased step size has to be used for TDE to converge and a slower convergence speed cannot be avoided as the feedback delay increases. Compared with the data-aided LMS-based method, the CMA-based method has a slower convergence speed and larger variation after convergence. Similar results are confirmed using numerical simulations for fiber dispersive channels. As the step size increases, a feedback delay of 20 clock cycles might cause the TDE to diverge. Compared with the CMA-based method, the LMS-based method has a higher tolerance on the feedback delay and allows a larger step size for a faster convergence speed. © *The Authors. Published by SPIE under a Creative Commons Attribution 3.0 Unported License. Distribution or reproduction of this work in whole or in part requires full attribution of the original publication, including its DOI.* [DOI: 10.1117/1.OE.55.4.046110]

1 Introduction

Higher-level modulation schemes like polarization-division multiplexed quadrature-phase-shift-keying (PDM-QPSK) have been widely used for high-speed optical fiber communication systems with transmission rate of 100 Gb/s and above for higher spectrum efficiency.[1–3] Coherent optical receivers are required to recover the phase information included in such modulation schemes.[4–6] Instead of using dispersion compensation fiber or optical phase conjugation for fiber dispersion compensation, digital optical coherent receivers with digital channel equalizer have become the dominating choice due to its high flexibility and low cost.

Digital signal processing modules to fulfill channel equalization, carrier phase estimation, and frequency offset estimation are the keys for the implementation of digital optical coherent receivers.[7,8] The channel equalization for fiber dispersive channel can be implemented either in time-domain or in frequency-domain. For long-fiber transmission length with large amount of accumulated fiber dispersion, a frequency-domain equalizer is more efficient due to its low complexity and high parallel implementation of fast Fourier transform.[9,10] However, an accurate estimation on the accumulated fiber dispersion is required.[11,12] Instead, a time-domain equalizer (TDE) can achieve adaptation following the time-varying channel degradation through the iteration on its tap coefficients.

The iterative updating on the tap coefficient is of great importance for the correct working of an adaptive TDE. The data-aided least-mean square (LMS)-based method and the nondata-aided constant modulus algorithm (CMA)-based method are the two most commonly used ways.[13–15] Though there have been a lot of research on the electrical channel equalizers based on simulation or off-line experiments,[16–18] the real-time implementation of such digital equalizers for 100 Gb/s and above rate is difficult due to the bottleneck of the hardware processing speed not available from current chip technology.[19] The computation delay on the error signal feedback from the parallel and pipelined implementation was found to have detrimental effects on the convergence performance of the adaptive TDE.[20–22]

This paper focuses on the effects of the feedback delay on the TDE's convergence speed and performance. Section 2 gives a brief introduction to the principle of the TDE studied in this paper. In Sec. 3, a simplified theoretical method is proposed to study the effect of the feedback delay for both LMS- and CMA-based methods, where the mean value and the variance of the tap coefficients are derived. Section 4 compares the convergence performance between the LMS- and CMA-based methods for different step sizes and feedback delays. Numerical simulations are used to verify the results for fiber dispersive channels in Sec. 5. Section 6 concludes the paper.

2 Principle of Time-Domain Equalizer

The schematic of an adaptive TDE with LMS-based method for coefficient updating is shown in Fig. 1. r_k is the received

---

*Address all correspondence to: Bo Xu, E-mail: xubo@uestc.edu.cn
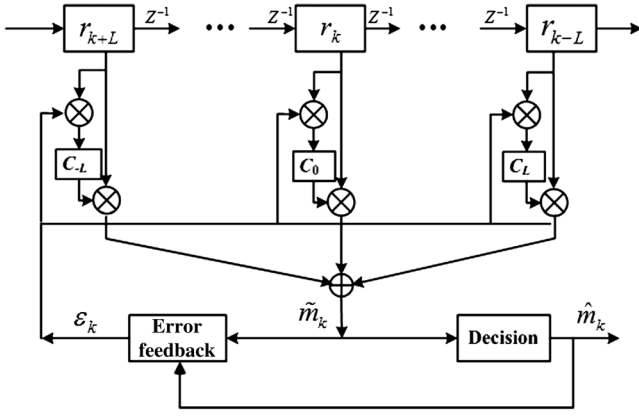
Fig. 1 Schematic of an adaptive TDE.

signal and $\tilde{m}_k$ is the output after equalization. $\varepsilon_k = \tilde{m}_k - \hat{m}_k$ is the error signal used as a feedback in the adaptation. In practical high-speed optical fiber communication systems, higher-order modulation schemes like QPSK together with polarization-division multiplexing are used to increase the spectrum efficiency. At the digital optical coherent receiver, a butterfly-structured TDE with four subequalizers is commonly used for simultaneous dispersion compensation and polarization-division demultiplexing. Assume that the four subequalizers are named Hxx, Hxy, Hyx, and Hyy, the outputs of the subequalizers can be written as a convolution between the received signals and the tap coefficients of the equalizer as

$$\tilde{m}_{xx,k} = \sum_{l=-L}^{L} C_{xx,l} r_{x,k-l}, \quad \tilde{m}_{yx,k} = \sum_{l=-L}^{L} C_{yx,l} r_{y,k-l}$$

$$\tilde{m}_{xy,k} = \sum_{l=-L}^{L} C_{xy,l} r_{x,k-l}, \quad \tilde{m}_{yy,k} = \sum_{l=-L}^{L} C_{yy,l} r_{y,k-l}. \quad (1)$$

In Eq. (1), $r_{x,k} = I_{x,k} + jQ_{x,k}$ is the received signal on the X-polarization and $r_{y,k} = I_{y,k} + jQ_{y,k}$ is the received signal on the Y-polarization. $\tilde{m}_{x,k} = \tilde{m}_{xx,k} + \tilde{m}_{yx,k}$ and $\tilde{m}_{y,k} = \tilde{m}_{xy,k} + \tilde{m}_{yy,k}$ are the final outputs from the butterfly TDE on the two polarizations for the k'th time slot. Here, it is assumed that the four subequalizers all have the same number of the tap coefficients, $2L + 1$.

LMS algorithm is a commonly used data-aided method for tap coefficients' updating for adaptive TDEs. For this case, error signals used as feedback signals in the iteration are computed as

$$\varepsilon_{x,k} = \tilde{m}_{x,k} - \hat{m}_{x,k}, \qquad \varepsilon_{y,k} = \tilde{m}_{y,k} - \hat{m}_{y,k}, \quad (2)$$

where $\hat{m}_{x,k}$ and $\hat{m}_{y,k}$ are the decision results for the k'th time slot. Then, take the subequalizer Hxx as an example, its tap coefficients are updated as

$$C_{xx}[k+1] = C_{xx}[k] - \lambda \varepsilon_{x,k} \cdot r_{x,k}^*, \quad (3)$$

where λ is a step size parameter, C_{xx} is the coefficient vector from the $2L + 1$ taps, and $r_{x,k}$ is the received signal vector used to compute $\tilde{m}_{xx,k}$. It is known from Eqs. (1)–(3) that both the equalizers' output computation and the tap

coefficient updating involve complex multiplication and addition. Taking into account that the signal is sampled at a sampling rate of 56G-samples per second at the digital optical coherent receiver, it is impossible to implement the required complex multiplication and addition in a serial way with current application specific integrated circuits technology in real-time implementation. Parallel implementation is necessary together with a pipelined structure where different logic units are used for different computations like multiplication or addition. Registers are used between different logic units for signal buffering. Though a higher clock rate can be achieved with the parallel and pipelined implementation, computation delay cannot be avoided between the input signals and the error feedback signals for tap coefficient iteration.

Under the assumption that D clock cycles are required to compute the error feedback signal from the input signals, the LMS-based updating equation for the TDE becomes

$$C_{xx}[k+1] = C_{xx}[k] - \lambda \varepsilon_{x,k-D} \cdot r_{x,k-D}^*. \quad (4)$$

Such a computation delay will have great influence on the convergence speed and performance of the TDE.

CMA is another commonly used method for tap coefficients' updating for adaptive TDE. The error feedback signal for CMA becomes

$$\varepsilon_{x,k} = R_2 - |\tilde{m}_{x,k}|^2, \quad (5)$$

where R_2 is a parameter defined as $R_2 = E[|a(k)|^4]/E[|a(k)|^2]$. For QPSK modulation, $R_2 = 1$ and the corresponding iteration equation is

$$C_{xx}[k+1] = C_{xx}[k] + \lambda \varepsilon_{x,k-D} \cdot r_{x,k-D}^* \cdot \tilde{m}_{x,k-D}. \quad (6)$$

For the ideal case without error feedback delay, $D = 0$. A longer computation delay is expected for CMA-based method due to the fact that its iteration includes more complex computations than the LMS-based method.

3 Analysis on the Feedback Delay Effect

To study the effect of the feedback delay on the convergence performance of the TDE, this section proposes a simplified theoretical model under which the convergence speed and the variance of the coefficients can be derived for both LMS- and CMA-based methods with different feedback delays. Suppose that the signal is transmitted on a simplified channel model as

$$r_k = \alpha x_k + n_k, \quad (7)$$

where α is an unknown channel attenuation between the transmitted signal x_k and the received signal r_k, and n_k is the noise introduced by the channel. A channel equalizer with a single tap C_k is used to estimate and compensate for the channel attenuation, and the output of the equalizer is simply $y_k = C_k \times r_k$. The tap coefficient C_k is updated with either LMS- or CMA-based method.

First, we study the case with LMS-based method for the tap coefficient updating. For the ideal case without feedback delay, the updating equation is

$$C_{k+1} = C_k - \lambda \varepsilon_k \cdot r_k^*$$
$$= C_k - \lambda(\alpha C_k x_k + C_k n_k - x_k) \cdot (\alpha x_k + n_k). \quad (8)$$

Define that $C_k = \bar{C}_k + \Delta_k$, where $\bar{C}_k$ is the mean value of the tap coefficient at the k'th iteration and Δ_k is the variation of the tap coefficient due to channel noise. It is clear that the variance of the tap coefficient is $\sigma_k^2 = E\{\Delta_k^2\}$.

By substituting $C_k = \bar{C}_k + \Delta_k$ into Eq. (8), the iteration equations for the mean value and the variance of the tap coefficient are found to be

$$\bar{C}_{k+1} = \bar{C}_k + \alpha \cdot \lambda - \lambda(\alpha^2 + \sigma_0^2)\bar{C}_k, \quad (9)$$

$$\sigma_{k+1}^2 = \{(1 - \alpha^2\lambda)^2 + (6\alpha^2\lambda^2 - 2\lambda)\sigma_0^2 + 3\lambda^2\sigma_0^4\}\sigma_k^2$$
$$+ 4\alpha\lambda^2\bar{C}_k(\alpha\bar{C}_k - 1)\sigma_0^2 + \lambda^2\sigma_0^2 + 2\lambda^2\bar{C}_k^2\sigma_0^4, \quad (10)$$

where σ_0^2 is the variance of channel noise n_k.

However, if there exists a non-negligible feedback delay of D clock cycles, the above coefficient updating equation becomes

$$C_{k+1} = C_k - \lambda(\alpha C_{k-D}x_{k-D} + C_{k-D}n_{k-D} - x_{k-D})$$
$$\cdot (\alpha x_{k-D} + n_{k-D}). \quad (11)$$

The corresponding iteration equations for the mean and the variance of the tap coefficient are obtained as

$$\bar{C}_{k+1} = \bar{C}_k + \alpha \cdot \lambda - \lambda(\alpha^2 + \sigma_0^2)\bar{C}_{k-D}, \quad (12)$$

$$\sigma_{k+1}^2 = \sigma_k^2 + \alpha^4\lambda^2\sigma_{k-D}^2 + \lambda^2\sigma_0^2 + 4\alpha^2\lambda^2\bar{C}_{k-D}^2\sigma_0^2$$
$$+ 6\alpha^2\lambda^2\sigma_{k-D}^2\sigma_0^2 - 4\alpha\lambda^2\bar{C}_{k-D}\sigma_0^2 + 2\lambda^2\bar{C}_{k-D}^2\sigma_0^4$$
$$+ 3\lambda^2\sigma_{k-D}^2\sigma_0^4 - 2\alpha^2\lambda E\{\Delta_k\Delta_{k-D}\}$$
$$- 2\lambda\sigma_0^2 E\{\Delta_k\Delta_{k-D}\}. \quad (13)$$

The key to compute σ_{k+1}^2 is to compute $E\{\Delta_k\Delta_{k-D}\}$, which can be computed iteratively as

$$E\{\Delta_{k-D+1}\Delta_{k-D}\} = \sigma_{k-D}^2 - \lambda(\alpha^2 + \sigma_0^2)E\{\Delta_{k-D}\Delta_{k-2D}\}$$
$$E\{\Delta_{k-D+2}\Delta_{k-D}\} = E\{\Delta_{k-D+1}\Delta_{k-D}\}$$
$$- \lambda(\alpha^2 + \sigma_0^2)E\{\Delta_{k-D}\Delta_{k-2D+1}\}$$

$$\cdots$$

$$E\{\Delta_{k-1}\Delta_{k-D}\} = E\{\Delta_{k-2}\Delta_{k-D}\}$$
$$- \lambda(\alpha^2 + \sigma_0^2)E\{\Delta_{k-D}\Delta_{k-2D-2}\}$$
$$E\{\Delta_k\Delta_{k-D}\} = E\{\Delta_{k-1}\Delta_{k-D}\} - \lambda(\alpha^2 + \sigma_0^2)E\{\Delta_{k-D}\Delta_{k-2D-1}\}. \quad (14)$$

Next, the tap coefficient updating with CMA-based method is derived. For the ideal case without feedback delay, the updating equation with the CMA-based method is

$$C_{k+1} = C_k + \lambda \varepsilon_k \cdot \tilde{m}_k \cdot r_k^*$$
$$= C_k + \lambda C_k(\alpha x_k + n_k)^2 - \lambda C_k^3(\alpha x_k + n_k)^4. \quad (15)$$

The mean value of the tap coefficient during the iteration is

$$\bar{C}_{k+1} = \bar{C}_k + \alpha^2\lambda\bar{C}_k - \lambda\alpha^4\bar{C}_k^3 + \lambda\bar{C}_k\sigma_0^2$$
$$- 6\alpha^2\lambda\bar{C}_k^3\sigma_0^2 - 3\lambda\bar{C}_k^3\sigma_0^4. \quad (16)$$

and

$$C_{k+1} = (\bar{C}_k + \Delta_k) + \lambda(\bar{C}_k + \Delta_k)(\alpha x_k + n_k)^2$$
$$- \lambda(\bar{C}_k + \Delta_k)^3(\alpha x_k + n_k)^4$$
$$= (\bar{C}_k + \Delta_k) + \lambda(\bar{C}_k + \Delta_k)(\alpha x_k + n_k)^2$$
$$- \lambda(\bar{C}_k^3 + 3\bar{C}_k^2\Delta_k + 3\bar{C}_k\Delta_k^2 + \Delta_k^3)(\alpha x_k + n_k)^4. \quad (17)$$

It is observed that the computation of the $E\{\Delta_{k+1}^2\}$ requires higher-order moments like $E\{\Delta_k^4\}$, $E\{\Delta_k^6\}$, and so on. Under the assumption that the coefficient variation is small compared with its mean value after the tap coefficient converges, the higher-order terms of the variation in Eq. (17) are ignored to obtain a tractable result on the coefficient variance as

$$\sigma_{k+1}^2 = 96 \cdot \lambda^2 \cdot \bar{C}_k^6 \cdot \sigma_0^8 + 384 \cdot \alpha^2 \cdot \lambda^2 \cdot \bar{C}_k^6 \cdot \sigma_0^6$$
$$+ 168 \cdot \alpha^4 \cdot \lambda^2 \cdot \bar{C}_k^6 \cdot \sigma_0^4 + 16 \cdot \alpha^6 \cdot \lambda^2 \cdot \bar{C}_k^6 \cdot \sigma_0^2$$
$$+ 945 \cdot \lambda^2 \cdot \bar{C}_k^4 \cdot \sigma_0^8 \cdot \sigma_k^2 + 3780 \cdot \alpha^2 \cdot \lambda^2 \cdot \bar{C}_k^4 \cdot \sigma_0^6 \cdot \sigma_k^2$$
$$+ 1890 \cdot \alpha^4 \cdot \lambda^2 \cdot \bar{C}_k^4 \cdot \sigma_0^4 \cdot \sigma_k^2$$
$$+ 252 \cdot \alpha^6 \cdot \lambda^2 \cdot \bar{C}_k^4 \cdot \sigma_0^2 \cdot \sigma_k^2 + 9 \cdot \alpha^8 \cdot \lambda^2 \cdot \bar{C}_k^4 \cdot \sigma_k^2$$
$$- 24 \cdot \lambda^2 \cdot \bar{C}_k^4 \cdot \sigma_0^6 - 72 \cdot \alpha^2 \cdot \lambda^2 \cdot \bar{C}_k^4 \cdot \sigma_0^4$$
$$- 16 \cdot \alpha^4 \cdot \lambda^2 \cdot \bar{C}_k^4 \cdot \sigma_0^2 - 90 \cdot \lambda^2 \cdot \bar{C}_k^2 \cdot \sigma_0^2 \cdot \sigma_k^6$$
$$- 270 \cdot \alpha^2 \cdot \lambda^2 \cdot \bar{C}_k^2 \cdot \sigma_0^4 \cdot \sigma_k^2$$
$$- 18 \cdot \lambda \cdot \bar{C}_k^2 \cdot \sigma_0^4 \cdot \sigma_k^2 - 90 \cdot \alpha^4\lambda^2 \cdot \bar{C}_k^2 \cdot \sigma_0^2 \cdot \sigma_k^2$$
$$- 36 \cdot \alpha^2 \cdot \lambda \cdot \bar{C}_k^2 \cdot \sigma_0^2 \cdot \sigma_k^2$$
$$- 6 \cdot \alpha^6 \cdot \lambda^2 \cdot \bar{C}_k^2 \cdot \sigma_k^2 - 6 \cdot \alpha^4 \cdot \lambda \cdot \bar{C}_k^2 \cdot \sigma_k^2$$
$$+ 2 \cdot \lambda^2 \cdot \sigma_0^4 \cdot \sigma_k^2 + 4 \cdot \alpha^2 \cdot \lambda^2 \cdot \bar{C}_k^2 \cdot \sigma_0^2$$
$$+ 3 \cdot \lambda^2 \cdot \sigma_0^4 \cdot \sigma_k^2 + 6 \cdot \alpha^2 \cdot \lambda^2 \cdot \sigma_0^2 \cdot \sigma_k^2$$
$$+ 2 \cdot \lambda \cdot \sigma_0^2 \cdot \sigma_k^2 + \alpha^4 \cdot \lambda^2 \cdot \sigma_k^2 + 2 \cdot \alpha^2 \cdot \lambda \cdot \sigma_k^2 + \sigma_k^2. \quad (18)$$

For the case with feedback delays, the above iteration equations become

$$C_{k+1} = C_k + \lambda\varepsilon_{k-D} \cdot \tilde{m}_{k-D} \cdot r_{k-D}^*$$
$$= C_k + \lambda C_{k-D}(\alpha x_{k-D} + n_{k-D})^2 - \lambda C_{k-D}^3(\alpha x_{k-D} + n_{k-D})^4, \quad (19)$$

$$\bar{C}_{k+1} = \bar{C}_k + \alpha^2\lambda\bar{C}_{k-D} - \alpha^4\lambda\bar{C}_{k-D}^3 + \lambda\bar{C}_k\sigma_0^2$$
$$- 6\alpha^2\lambda\bar{C}_{k-D}^3\sigma_0^2 - 3\lambda\bar{C}_{k-D}^3\sigma_0^4, \quad (20)$$
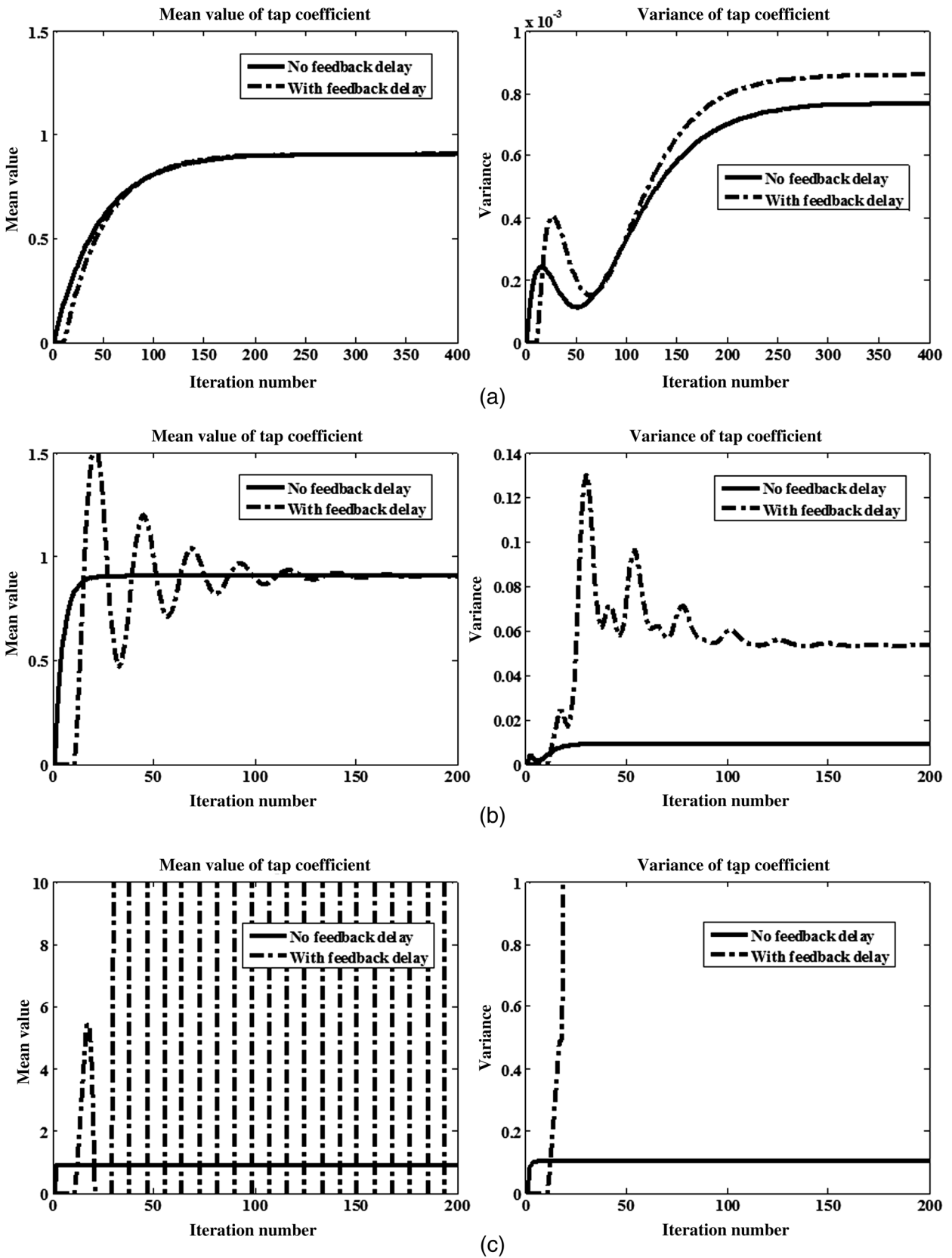
Fig. 2 The mean value and the variance of the tap coefficient for the LMS-based method with different step sizes: (a) $\lambda = 0.02$, (b) $\lambda = 0.2$, and (c) $\lambda = 0.9$.

$$
\begin{aligned}
\sigma_{k+1}^2 = {} & \sigma_k^2 - \lambda \cdot E\{\Delta_k \Delta_{k-D}\} \cdot (18 \cdot \bar{C}_{k-D} \cdot \sigma_0^4 + 36 \cdot \alpha^2 \\
& \cdot \bar{C}_{k-D}^2 \cdot \sigma_0^2 + 6 \cdot \alpha^4 \cdot \bar{C}_{k-D}^2 - 2 \cdot \sigma_0^2 - 2 \cdot \alpha^2) \\
& + \alpha^4 \cdot \lambda^2 \cdot \sigma_{k-D}^2 - 6 \cdot \alpha^6 \cdot \lambda^2 \cdot \bar{C}_{k-D}^2 \cdot \sigma_{k-D}^2 \\
& + 9 \cdot \alpha^8 \cdot \lambda^2 \cdot \bar{C}_{k-D}^4 \cdot \sigma_{k-D}^2 + 4 \cdot \alpha^2 \cdot \lambda^2 \cdot \bar{C}_{k-D}^2 \cdot \sigma_0^2 \\
& + 2 \cdot \lambda^2 \cdot \bar{C}_{k-D}^2 \cdot \sigma_0^4 - 16 \cdot \alpha^4 \cdot \lambda^2 \cdot \bar{C}_{k-D}^4 \cdot \sigma_0^2 \\
& - 72 \cdot \lambda^2 \cdot \bar{C}_{k-D}^4 \cdot \sigma_0^4 + 16 \cdot \alpha^6 \cdot \lambda^2 \cdot \bar{C}_{k-D}^6 \cdot \sigma_0^2 \\
& - 24 \cdot \lambda^2 \cdot \bar{C}_{k-D}^4 \cdot \sigma_0^6 + 168 \cdot \alpha^4 \cdot \lambda^2 \cdot \bar{C}_{k-D}^6 \cdot \sigma_0^4 \\
& + 384 \cdot \alpha^2 \cdot \lambda^2 \cdot \bar{C}_{k-D}^6 \cdot \sigma_0^6 + 96 \cdot \lambda^2 \cdot \bar{C}_{k-D}^6 \cdot \sigma_0^8 \\
& + 6 \cdot \alpha^2 \cdot \lambda^2 \cdot \sigma_{k-D}^2 \cdot \sigma_0^2 + 3 \cdot \lambda^2 \cdot \sigma_{k-D}^2 \cdot \sigma_0^4 \\
& - 90 \cdot \lambda^2 \cdot \bar{C}_{k-D}^2 \cdot \sigma_{k-D}^2 \cdot \sigma_0^6 \\
& - 90 \cdot \alpha^4 \cdot \lambda^2 \cdot \bar{C}_{k-D}^2 \cdot \sigma_{k-D}^2 \cdot \sigma_0^2 \\
& - 270 \cdot \alpha^2 \cdot \lambda^2 \cdot \bar{C}_{k-D}^2 \cdot \sigma_{k-D}^2 \cdot \sigma_0^4 \\
& + 252 \cdot \alpha^6 \cdot \lambda^2 \cdot \bar{C}_{k-D}^2 \cdot \sigma_{k-D}^2 \cdot \sigma_0^2 \\
& + 1890 \cdot \alpha^4 \cdot \lambda^2 \cdot \bar{C}_{k-D}^4 \cdot \sigma_{k-D}^2 \cdot \sigma_0^4 \\
& + 3780 \cdot \alpha^2 \cdot \lambda^2 \cdot \bar{C}_{k-D}^4 \cdot \sigma_{k-D}^2 \cdot \sigma_0^6 \\
& + 945 \cdot \lambda^2 \cdot \bar{C}_{k-D}^4 \cdot \sigma_{k-D}^2 \cdot \sigma_0^8.
\end{aligned}
\tag{21}
$$

4 Effects of the Feedback Delay on Equalizer Convergence

The step size is an important parameter for the design of an adaptive TDE. A larger step size is usually preferred for a faster convergence speed. However, a too large step size might cause the TDE to diverge. Based on the above equations on the mean value and the variance of tap coefficient, a detailed comparison between the case with and without feedback delays is studied in the following for LMS- and CMA-based methods. In the following numerical analysis, the unknown channel attenuation is assumed to be 1.

Based on Eqs. (8)–(13), Fig. 2 gives the mean value and the variance of the coefficient iteration using different step sizes in the LMS-based method. The variance of the channel noise σ_0^2 is set to be 0.1, and the feedback delay D is fixed at five clock cycles. It is seen from the figure that a small step size of 0.02 has a slow convergence speed and a feedback delay of five clock cycles has negligible effect on the TDE's convergence with a slightly increased variance after convergence. As the step size is increased to 0.2, the TDE without feedback delay can achieve a faster convergence at a cost of increased variance after convergence when compared with a step size of 0.02. However, if there exists a feedback delay of five clock cycles, some oscillation is observed during the coefficient updating with increased variance when compared with the ideal case without feedback delay. When the step size is further increased to 0.9, the TDE can still converge under the ideal case. However, the mean value shows large oscillation for the case with feedback delay and the magnitude of the oscillation is increasing with the number of iteration. Apparently, the TDE is divergent for this case. Moreover, the variance of the tap coefficient for this case also grows to infinity with the number of iteration.

It is known from Fig. 2 that a much larger step size can be used for the adaptive TDE under the ideal case for the LMS-based method. However, if the feedback delay is non-negligible as in the practice, the step size has to be decreased to keep the TDE convergent, thus greatly reduces the convergence speed. Figure 3 shows the mean value and the variance of the coefficient under different feedback delays. The step size is fixed at 0.05 for all different feedback delays. As the feedback delay increases from 0 for the ideal case to 10 clock cycles, the TDE can still reach convergent at the cost of slowed down convergence speed and increased variance after convergence. However, if a feedback delay of 20 clock cycles is used, a strong oscillation is observed on both the mean value and the variance of the tap coefficient during the iteration.

Figure 4 gives the mean value and the variance of the tap coefficient for the CMA-based method using Eqs. (15)–(21). The same channel noise and feedback delay are used as in Fig. 2. For small step size of 0.02, a feedback delay of five clock cycles has negligible effect on the TDE's convergence at a cost of some increased variance. As the step size is increased to 0.06, a faster convergence can be achieved for both the ideal case and the case with feedback delay.
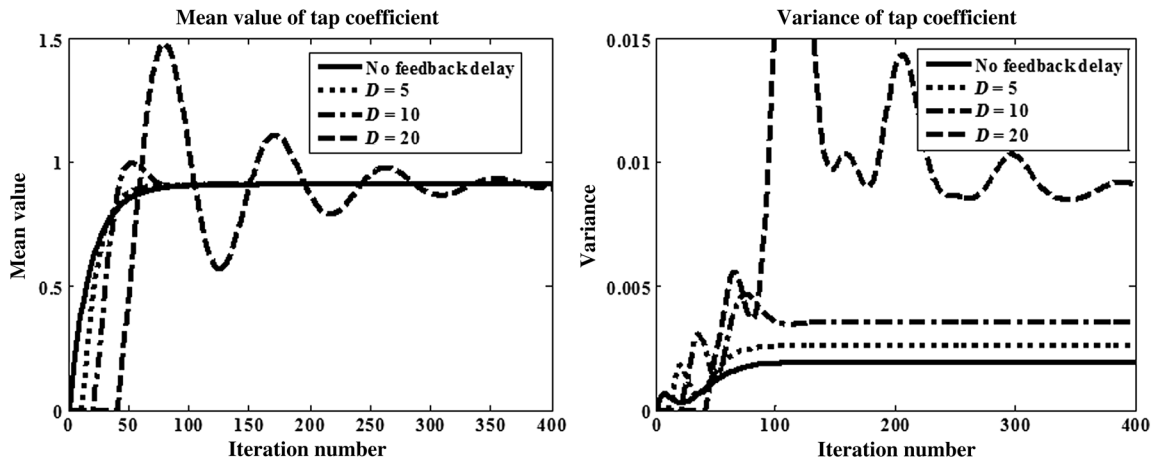
Fig. 3 The mean value and the variance of the tap coefficient for the LMS-based method with different feedback delays.
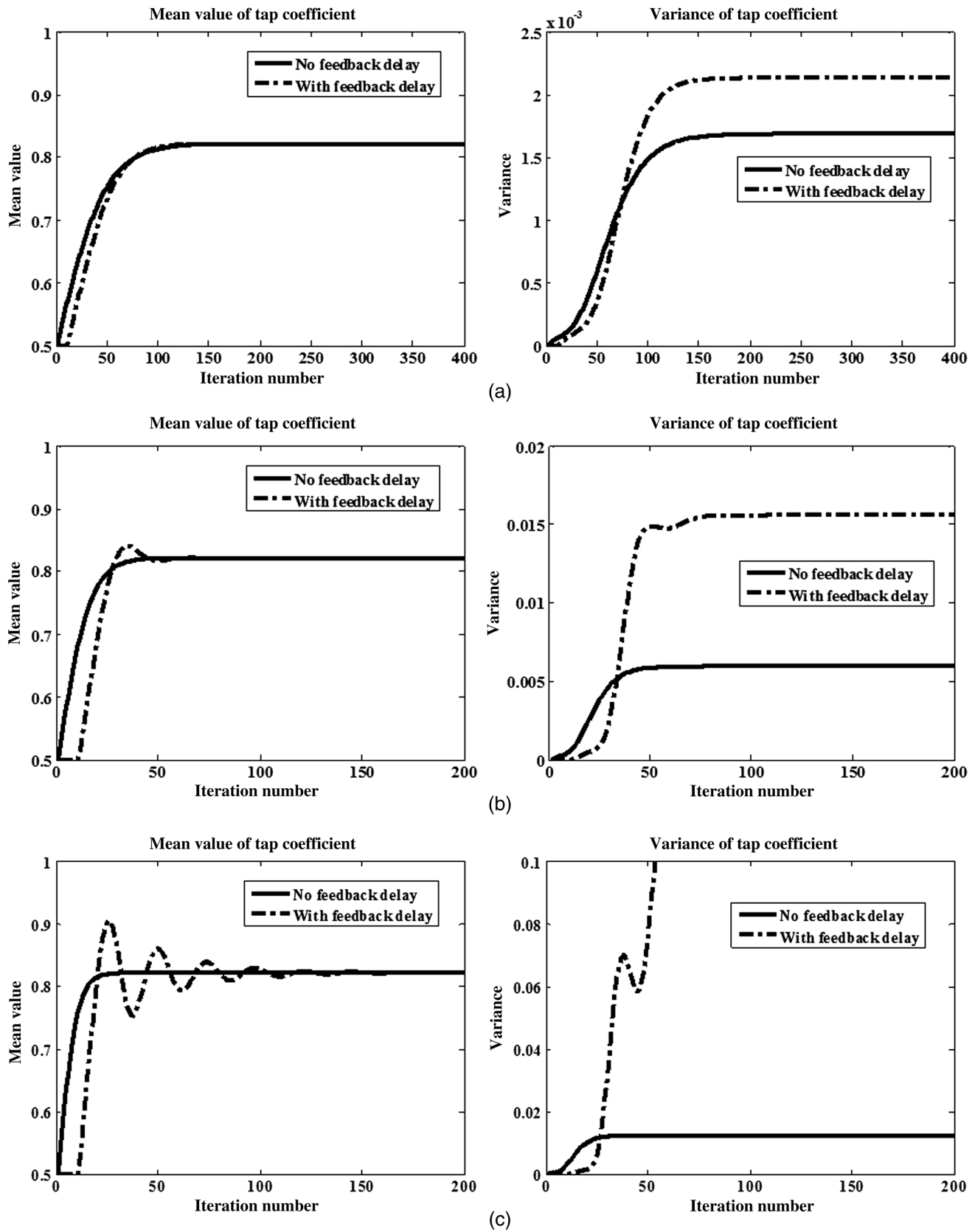
Fig. 4 The mean value and the variance of the tap coefficient for the CMA-based method with different step sizes: (a) $\lambda = 0.02$, (b) $\lambda = 0.06$, and (c) $\lambda = 0.1$.

However, the variance of the tap coefficient after convergence is more than doubled if there exists a feedback delay. If the step size is further increased to 0.1, the TDE can still converge for the ideal case. Instead, it is seen from the increasing variance of the tap coefficient that the TDE becomes divergent for the case with feedback delay.

Figure 5 shows the mean value and the variance of the coefficient for CMA-based method with different feedback delays. A step size of 0.03 is used in the computation. A similar behavior as the LMS-based method is observed. Negligible effect is found for small feedback delays. However, as the feedback delay is increased to 20 clock cycles, strong oscillation and divergence are also observed on both the mean value and the variance of the tap coefficient in the iteration.

Figure 6 compares the performance of the LMS- and CMA-based methods under two different cases: the ideal case and the case with a feedback delay of 10 clock cycles. For small step size of 0.02, both the LMS- and CMA-based methods can achieve convergence after about 100 iterations. After convergence, the LMS-based method has a better performance since the coefficient obtained using the LMS-based method has a smaller variance than the CMA-based method. For a relatively large step size of 0.1, the LMS-based method can achieve a faster convergence speed for both the ideal case and the case with feedback delay. For comparison, though the CMA-based method can still converge for the ideal case without feedback delay, it fails to converge for the case with feedback delay. A smaller step size is thus required for the CMA-based method than the LMS-based method which implies a slower convergence speed.

It is known from the above analysis that the feedback delay has great influence on the convergence performance of the adaptive equalizer no matter whether LMS- or CMA-based method is used. The larger the feedback delay is, the smaller the step size should be used in the iteration for the equalizer to converge. A comparison between the LMS- and the CMA-based methods is also made. Compared with the data-aided LMS-based method, a smaller step size is allowed for the nondata-aided CMA-based method when the same feedback delay is considered. A slower convergence speed is thus expected for the CMA-based method

together with a larger variance after convergence than the LMS-based method.

5 Simulation Results with Fiber Dispersive Channel

For a practical fiber dispersive channel, the feedback delay is also expected to have great impact on the TDE's convergence performance. Though closed-form expressions for the mean and the variance of the tap coefficients cannot be obtained for fiber dispersive channels, numerical simulations are used in this section to study the effects of feedback delay on the TDE convergence performance. PDM-QPSK signals with a bit rate of 112 Gb/s are assumed to transmit over 100 km uncompensated standard single-mode fiber in the simulations. For such a fiber transmission length, 22 taps are enough for the TDE.

Figure 7 shows the convergence performance under different feedback delays up to 20 clock cycles if a small step size of 0.02 is used in the iteration for both the LMS- and CMA-based methods. Such a small step size guarantees that the equalizers using both methods can achieve convergence. It is found that different values of feedback delay have negligible effects on the convergence performance no matter whether the LMS- or CMA-based method is used. However, there still exists obvious difference between the LMS- and the CMA-based methods where the data-aided LMS-based method is found to achieve a much faster convergence than the CMA-based method.

Similar behaviors as the previous section are observed as the step size is increased for a faster convergence speed. For the LMS-based method, Fig. 8 shows the convergence performance of the TDE using a step size of 0.12. For feedback delays less than 10 clock cycles, a faster convergence speed is obtained as compared with a small step size of 0.02. However, the TDE becomes divergent if the feedback delay is increased to 20 clock cycles. Figure 8 also shows the convergence performance of the TDE using a step size of 0.07 for the CMA-based method. Though the TDE can still reach convergence for small feedback delay less than 10 clock cycles, a large feedback delay of 20 clock cycles induces the TDE to diverge. Note that a smaller step size of 0.07 is used for the CMA-based method in Fig. 8 because
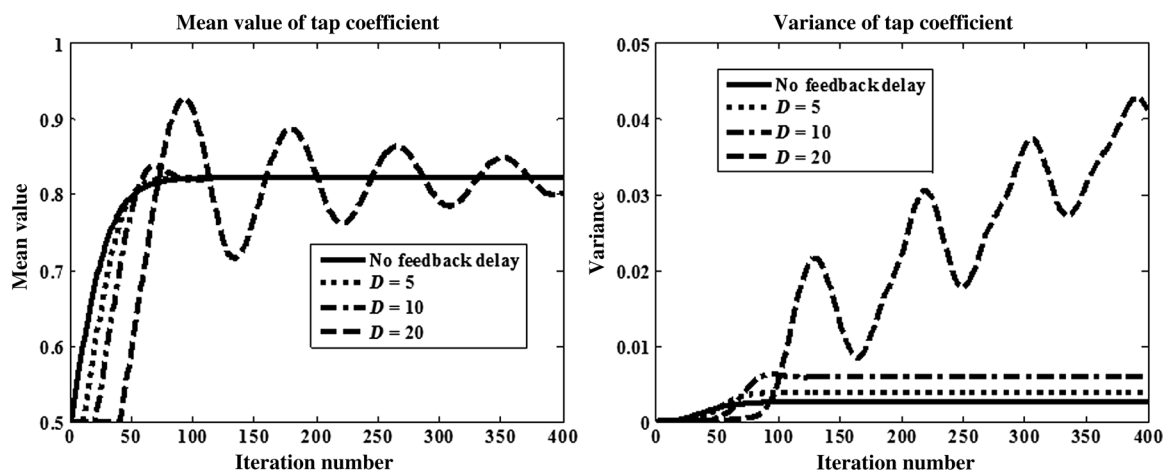
Fig. 5 The mean value and the variance of the tap coefficient for the CMA-based method with different feedback delays.
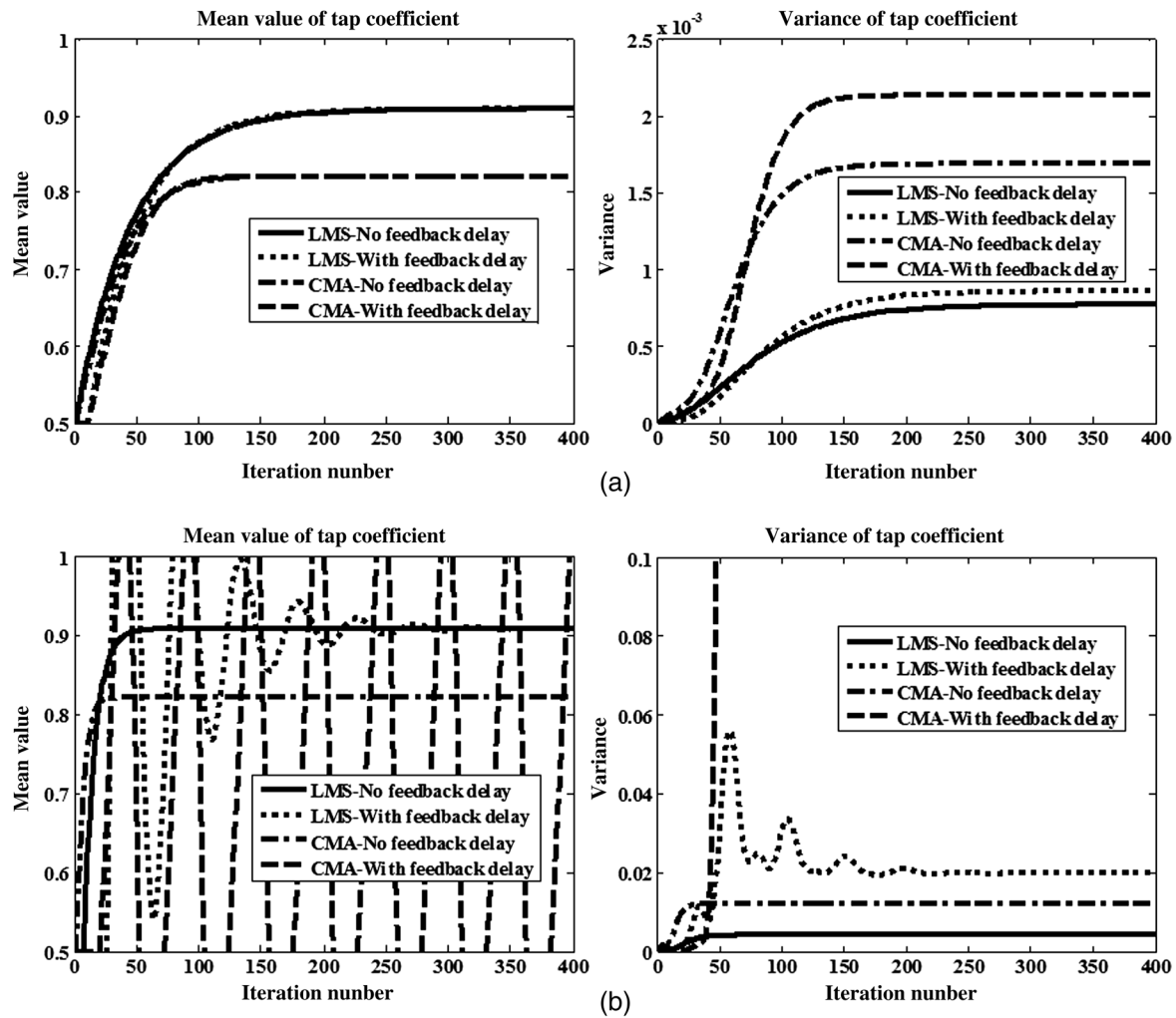
Fig. 6 Comparisons on the mean value and the variance of the tap coefficient for LMS- and CMA-based methods with different feedback delays: (a) $\lambda = 0.02$ and (b) $\lambda = 0.05$.
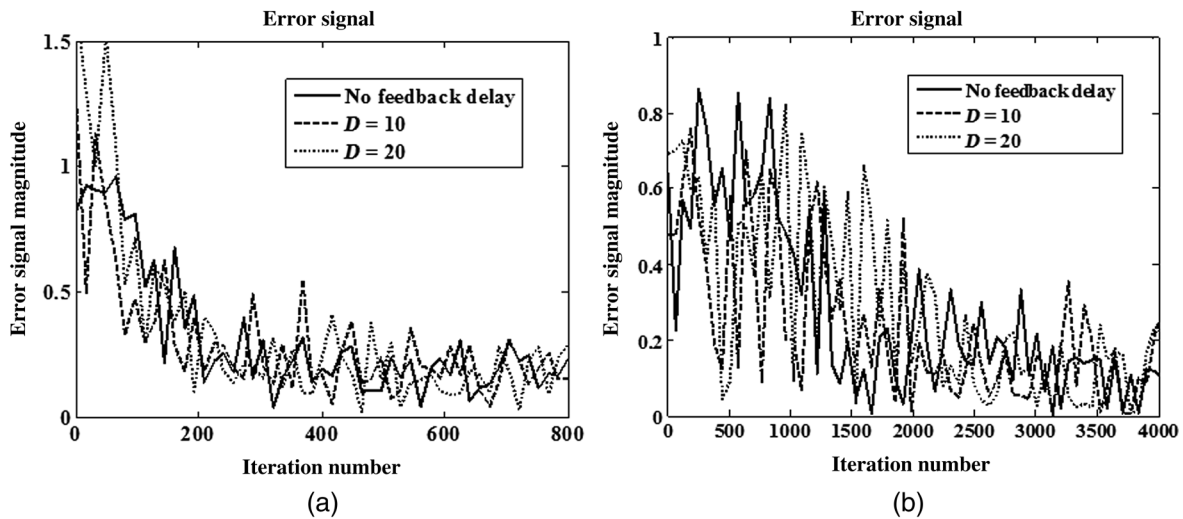
Fig. 7 Comparisons on the convergence performance for the LMS- and CMA-based methods with a small step size of 0.02 under different feedback delays for fiber dispersive channel: (a) LMS-based method and (b) CMA-based method.

Error signal

Error signal

(a)

(b)
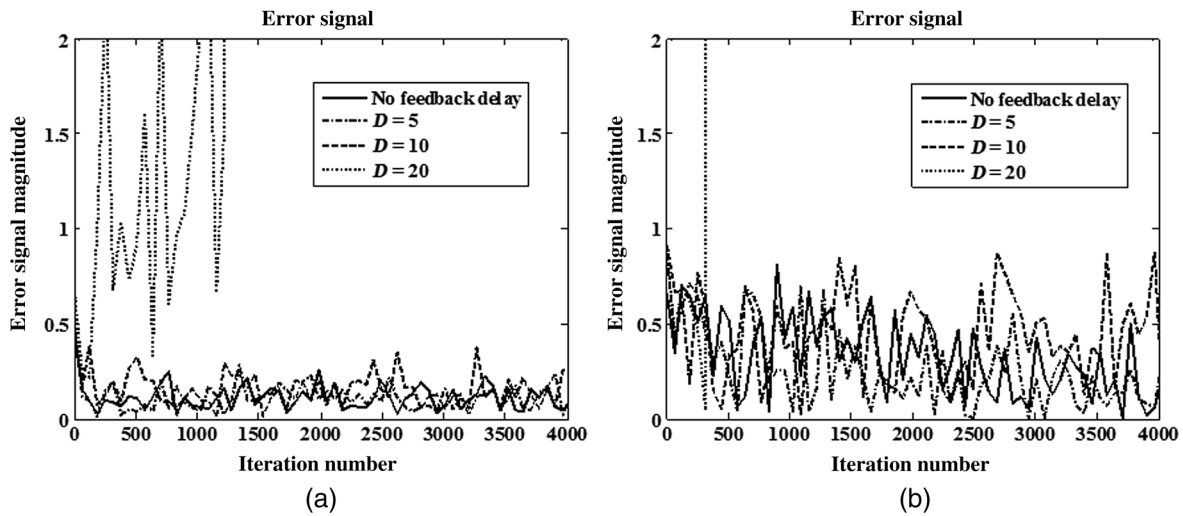
Fig. 8 Comparisons on the convergence performance for the LMS- and CMA-based methods with a larger step size under different feedback delays for fiber dispersive channel: (a) LMS-based method and (b) CMA-based method.

the same step size of 0.12 as in the LMS-based method causes the CMA-based method to diverge even at small feedback delay.

From the comparison on the different step sizes used in Fig. 8 for the LMS- and CMA-based methods, it is clear that the data-aided LMS-based method has a better tolerance on the effect of feedback delay if the step size is increased for faster convergence than the nondata-aided CMA-based method. For practical application in the equalizer design for digital optical coherent receiver, it is important to know the maximum allowed step size that can guarantee the convergence of the equalizer. For this purpose, Fig. 9 gives the simulation results on the maximum allowed step size for different feedback delays for both the LMS- and CMA-based methods. The same parameters as in Figs. 7 and 8 are used in the simulations. It is confirmed that a larger step size can be used for the data-aided LMS-based method than the nondata-aided CMA-based method.

Maximum allowed step size
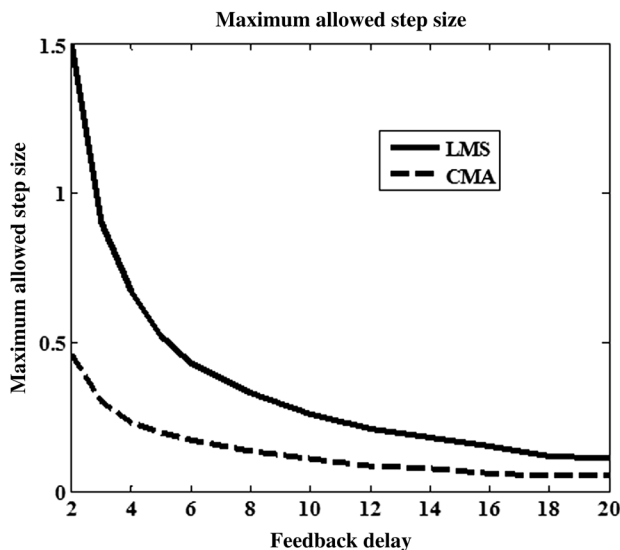
Fig. 9 Comparison on the maximum allowed step size between the LMS- and CMA-based methods for fiber dispersive channel.

6 Conclusions

Adaptive TDE is one of the most important modules for high-speed digital optical coherent receivers. For both the LMS- and CMA-based methods, the coefficient updating on the TDE requires computation of error signals as feedback. The feedback delay in practical implementation has serious impacts on the convergence performance of the TDE.

This paper proposes a simplified theoretical model based on which the mean value and the variance of the tap coefficient during iteration are derived for both the LMS- and CMA-based methods. The equation on variance is crucial for the study of the convergence performance of the adaptive TDE. Based on the equations, it is found that the existence of channel noise in the received signals might cause the tap coefficient to become divergent if a large step size is used. The effects of the feedback delay on the convergence performance are studied in detail for both LMS- and CMA-based methods using the theoretical results. It is found that as the feedback delay increases, a smaller step size has to be used for the TDE to converge and a slower convergence speed cannot be avoided. The CMA-based method has a slower convergence speed and larger variance after convergence, if the same step size is used as in the LMS-based method.

Based on numerical simulations, consistent results on the effects of the feedback delay on the TDE's convergence are obtained for fiber dispersive channel for both LMS- and CMA-based methods. For small step size, the feedback delay has negligible effect. However, as the step size increases for a faster convergence speed, a feedback delay of 20 clock cycles might cause the TDE to diverge. Compared with the CMA-based method, the data-aided LMS-based method has a higher tolerance on the feedback delay and allows a larger step size for faster convergence speed.

References

1. J. Zhang et al., "400 G transmission of super-Nyquist-filtered signal based on single-carrier 110-GBaud PDM QPSK with 100-GHz grid," *J. Lightwave Technol.* **32**(19), 3239–3246 (2014).
2. X. Li, J. Xiao, and J. Yu, "Heterodyne detection and transmission of 60-Gbaud PDM-QPSK signal with SE of 4 b/s/Hz," *Opt. Express* **22**(8), 9307–9313 (2014).
3. F. Zhang et al., "Fiber nonlinear tolerance comparison between 112 Gb/s coherent transmission systems using quadrature-phase-shift-keying, offset quadrature-phase-shift-keying, and minimum-shift-keying formats," *Opt. Eng.* **51**(10), 105001 (2012).
4. S. Zhang et al., "Performance study of 100-Gb/s super-Nyquist QPSK and Nyquist 8QAM over 25-GHz spacing," *IEEE Photonics Technol. Lett.* **27**(13), 1445–1448 (2015).
5. D. O. Otuya et al., "Single-channel 1.92 Tbit/s, Pol-Mux-64 QAM coherent Nyquist pulse transmission over 150 km with a spectral efficiency of 7.5 bit/s/Hz," *Opt. Express* **22**(20), 23776–23785 (2014).
6. V. R. Arbab and P. Saghari, "Effects of fiber impairments on constellation diagram of optical phase modulated signals," *Opt. Eng.* **51**(4), 045008 (2012).
7. S. M. Bilal et al., "Multistage carrier phase estimation algorithms for phase noise mitigation in 64-quadrature amplitude modulation optical systems," *J. Lightwave Technol.* **32**(17), 2973–2980 (2014).
8. X. Yi et al., "Impact of filter shape and bandwidth on terabit polarization-multiplexed quadrature phase-shift keying transmission with baud-rate spacing," *Opt. Eng.* **51**(10), 105005 (2012).
9. M. Kuschnerov et al., "DSP for coherent single-carrier receivers," *J. Lightwave Technol.* **27**(16), 3614–3622 (2009).
10. B. Spinnler, "Equalizer design and complexity for digital coherent receivers," *IEEE J. Sel. Top. Quantum Electron.* **16**(5), 1180–1192 (2010).
11. R. A. Soriano et al., "Chromatic dispersion estimation in digital coherent receivers," *J. Lightwave Technol.* **29**(11), 1627–1637 (2011).
12. R. Corsini et al., "Blind adaptive chromatic dispersion compensation and estimation for DSP-based coherent optical systems," *J. Lightwave Technol.* **31**(13), 2131–2139 (2013).
13. L.-D. Van and W.-S. Feng, "An efficient systolic architecture for the DLMS adaptive filter and its applications," *IEEE Trans. Circuits Syst. II* **48**(4), 359–366 (2001).
14. B. K. Mohanty and P. K. Meher, "Delayed block LMS algorithm and concurrent architecture for high-speed implementation of adaptive FIR filters," in *Proc. TENCON 2008 IEEE Region 10 Conf.* (2008).
15. K. Roberts et al., "Performance of dual-polarization QPSK for optical transport systems," *J. Lightwave Technol.* **27**(16), 3546–3559 (2009).
16. E. Pincemin et al., "Novel blind equalizer for coherent DP-BPSK transmission systems: theory and experiment," *IEEE Photonics Technol. Lett.* **25**(18), 1835–1838 (2013).
17. J. Fickers et al., "Decision-feedback equalization of bandwidth constrained N-WDM coherent optical communication systems," *J. Lightwave Technol.* **31**(10), 1529–1537 (2013).
18. F. Tian et al., "Experiment of 2.56-Tb/s, polarization division multiplexing return-to-zero 16-ary quadrature amplitude modulation, 25 GHz grid coherent optical wavelength division multiplexing, 800 km transmission based on optical comb in standard single-mode fiber," *Opt. Eng.* **52**(11), 116103 (2013).
19. K. Roberts et al., "100 G and beyond with digital coherent signal processing," *IEEE Commun. Mag.* **48**(7), 62–69 (2010).
20. X. Zhou and X. Chen, "Parallel implementation of all-digital timing recovery for high-speed and real-time optical coherent receivers," *Opt. Express* **19**(10), 9282–9295 (2011).
21. G. A. Clark, S. K. Mitra, and S. R. Parker, "Block implementation of adaptive digital filters," *IEEE Trans. Circuits Syst.* **28**(6), 584–592 (1981).
22. R. Haimi-Cohen, H. Herzberg, and Y. Be'ery, "Delayed adaptive LMS filtering: current results," in *Proc. Int. Conf. on Acoustics, Speech, and Signal Processing*, pp. 1273–1276 (1990).

Qun Guo is currently a graduate student at the University of Electronic Science and Technology of China, School of Communication and Information Engineering. His current research interests include high-speed optical fiber coherent communications and digital signal processing technologies for optical fiber communications.

Biographies for the other authors are not available.